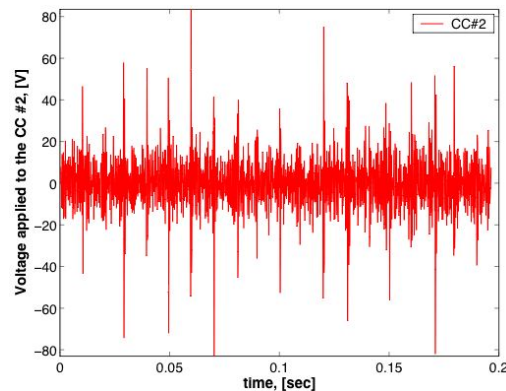


The Effects of Noise and Time Delay on RWM Feedback System Performance

O. Katsuro-Hopkins, J. Bialek, G. Navratil

*(Department of Applied Physics and Applied Mathematics,
Columbia University, New York, NY USA)*



9th workshop on MHD Stability Control
November 21-23, 2004



Outline

- Motivations
- Computer code **VALEN**
- Transient calculations for **DIII-D** with noise, time delay and low pass filter
- Time dependent problem for **HBT-EP** with time delay, band pass filter
- Conclusions



Motivations

- Control of long-wavelength MHD instabilities using conducting walls and external magnetic perturbations is a very promising route to improved reliability and better performance of magnetic confinement fusion devices. Control of these resistive wall slowed kink modes above the no-wall beta limit is essential to achieve bootstrap current sustained steady-state operation in a high gain tokamak fusion energy systems.
- The ability to accurately model and predict the performance of active MHD control systems is critical to present and future advanced confinement scenarios and machine design studies. The 3D VALEN modeling code has been designed and benchmarked to predict the performance limits of MHD control systems.



- To enhance VALEN's ability to model more realistic feedback systems initial value, time dependent capability, noise, time delay and finite bandwidth was added to the closed loop control system model.
- Presence of noise (white, Gaussian, $1/f$, etc.) in the RWM feedback system allows us to estimate feedback power requirements and system performance limits.



VALEN

*Developed by J. Bialek
and based on single mode model of A. Boozer*

**A Reliable Computational Tool For RWM
Passive and Active Control System Study**



The VALEN Equations

The VALEN matrix equations describing the conducting structure and mode and control coil geometry are for the unknowns $\{I^w\}$, $\{I^d\}$, and $\{I^p\}$ are:

$$[L_{ww}]\{I^w\} + [M_{wp}]\{I^d\} + [M_{wp}]\{I^p\} = \{\Phi_w\}$$

flux @ wall

$$[M_{pw}]\{I^w\} + [L_p]\{I^d\} + [L_p]\{I^p\} = \{\Phi\}$$

flux @ plasma

$$[L_p]\{I^p\} = [S]\{\Phi\}$$

stability equation

The equivalent circuit (induction) equations describing the system mode growth are then:

$$\{\dot{\Phi}_w\} + [R_{ww}]\{I^w\} = \{V\}$$

$$\{\dot{\Phi}\} + [R_d]\{I^d\} = \{0\}$$

Where $\{V\}$ depends on sensor signals $\{\Phi_s\}$ via the feedback loop equations:

$$\begin{bmatrix} [M_{sw}] & [M_{sd}] & [M_{sp}] \end{bmatrix} \begin{Bmatrix} \{I^w\} \\ \{I^d\} \\ \{I^p\} \end{Bmatrix} = \{\Phi_s\}$$

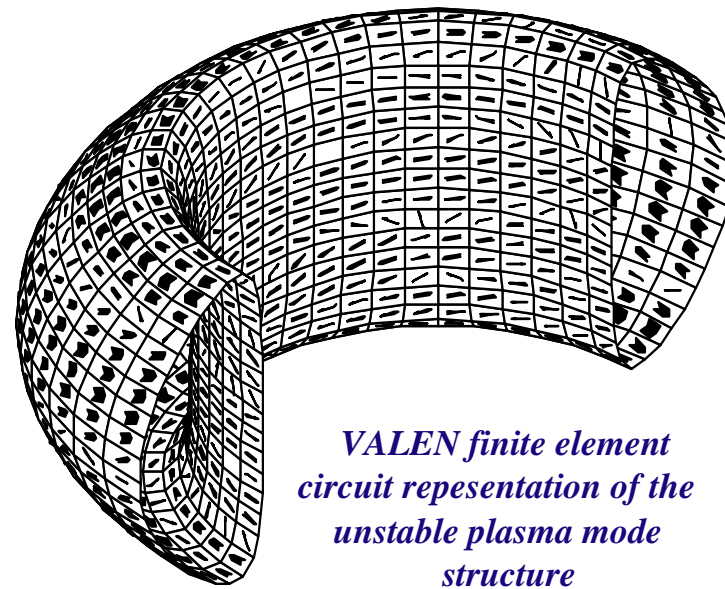
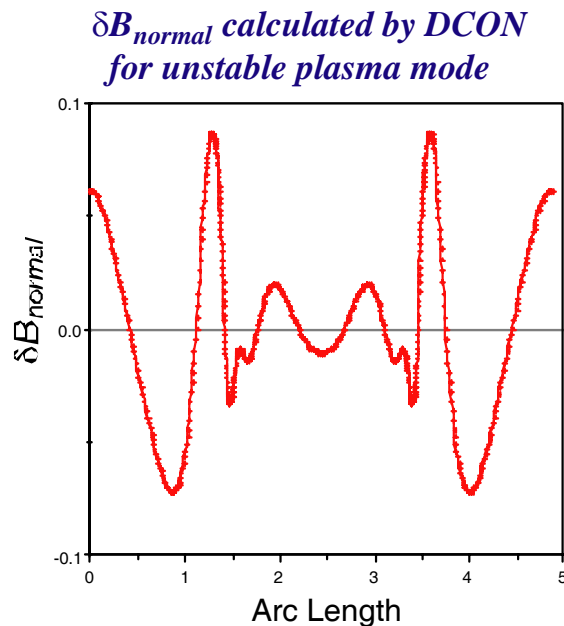


- **VALEN** uses **DCON** (A. Glasser) results without a conducting wall to formulate the stability equation
- Energy change $\delta W = 1/2 \sum \varpi_i \Phi_i^2$ in plasma & surroundings has negative eigenvalues ϖ_i if an instability exists, $f_i(\theta, \varphi)$ diagonalizes δW and defines the flux from the plasma instability $\Phi_i = \oint f_i(\theta, \varphi) \delta \vec{B} \cdot d\vec{a}$
- Complex helical magnetic geometry is expressed in terms of inductance and current $L_i = \Phi_i / I_i$ and the stability equation may be expressed as $S_{ij} = (\delta_{ij} + s_i \lambda_{ij})$ where $s_i = -\varpi_i L_i$ and the λ_{ij} may be derived from the $f_i(\theta, \varphi)$



VALEN Models External MHD Modes Determined by DCON As Surface Currents

- The interaction of an external MHD plasma instability with surrounding conductors and coils is completely described by giving δB_{normal} at the surface of the unperturbed plasma.
- VALEN uses this information in a circuit formulation of unstable plasma modes developed by Boozer to generate a finite element surface current representation of the unstable mode.

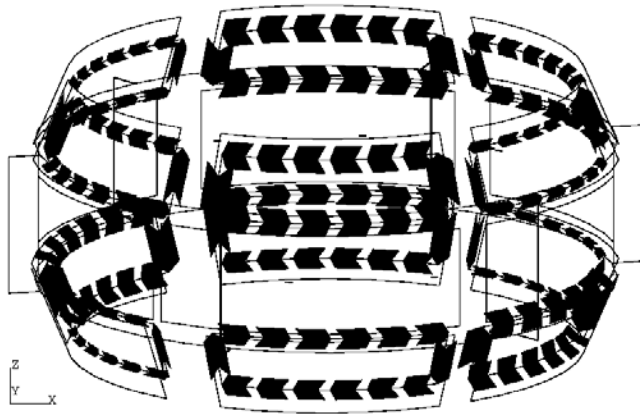


This methodology allows VALEN to use output plasma mode information from other instability physics codes (DCON, GATO, PEST or others)

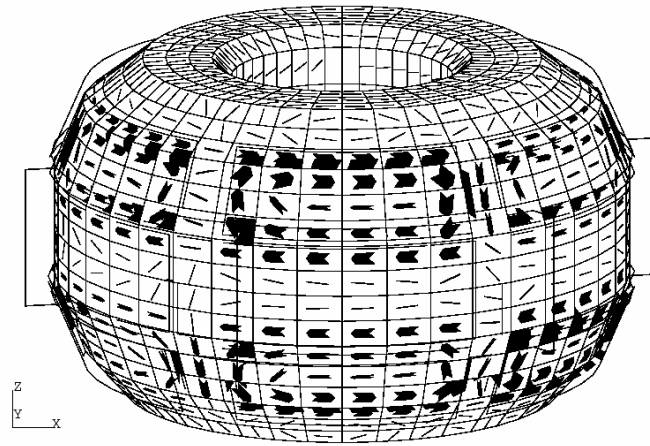
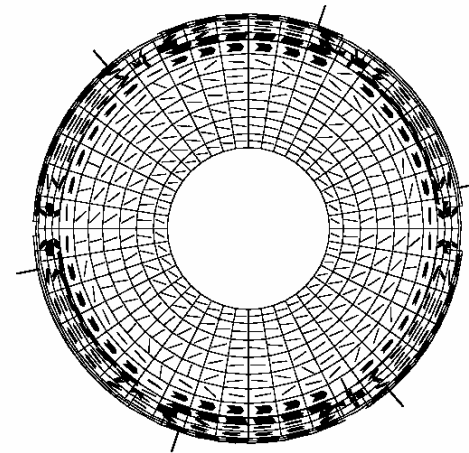


VALEN's 3D Finite Element Capability Is Important In Accurately Modeling Passive Wall Stabilization Limits and Active Feedback Performance

- Correct representation of the geometric details of vacuum chambers with portholes and passive stabilizing plates is required to determine RWM control limits
- VALEN calculates these effects and allows the design of optimized control systems with complicated real-world machine geometry



Eddy current pattern induced in the control coils in the DIII-D tokamak



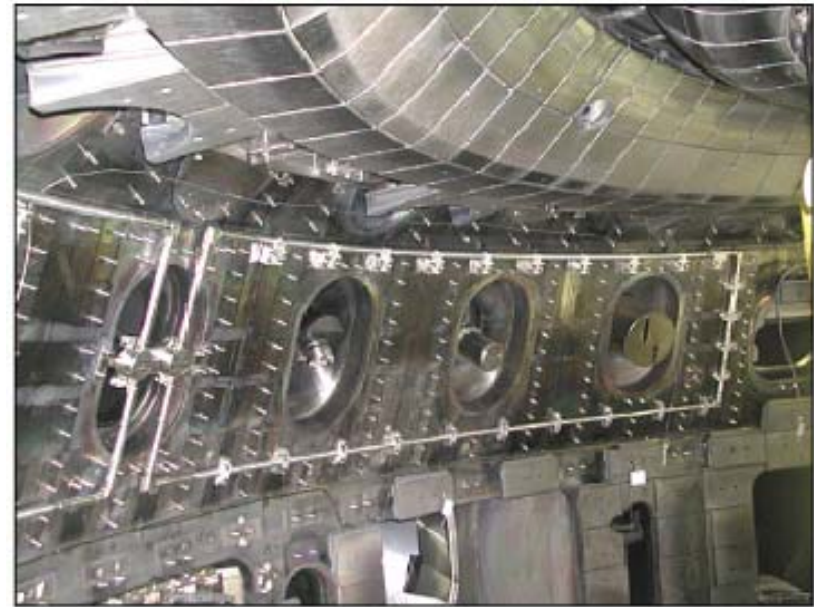
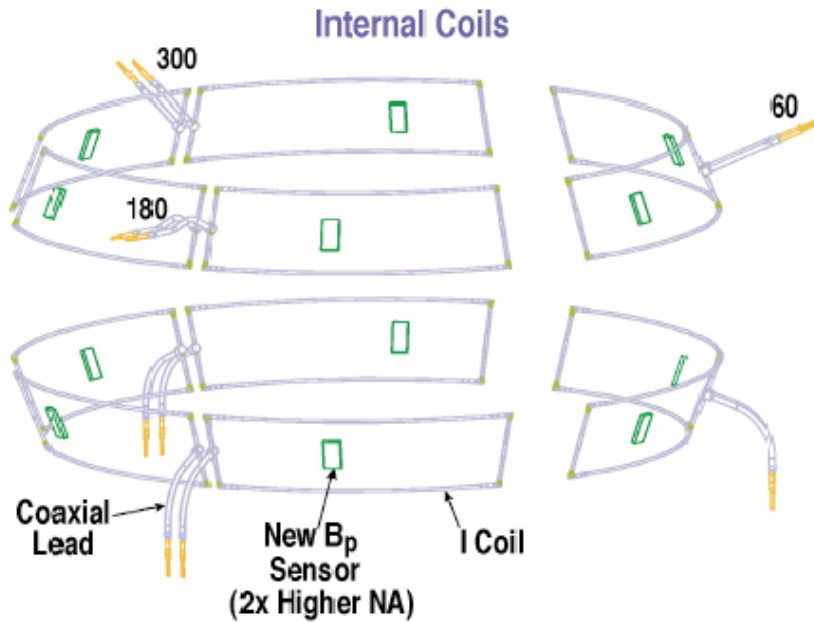
Eddy current pattern induced in the wall of the DIII-D tokamak due to an unstable $n=1$ RWM [top and side view]



Transient Calculations for **DIII-D** with noise, time delay and low pass filter

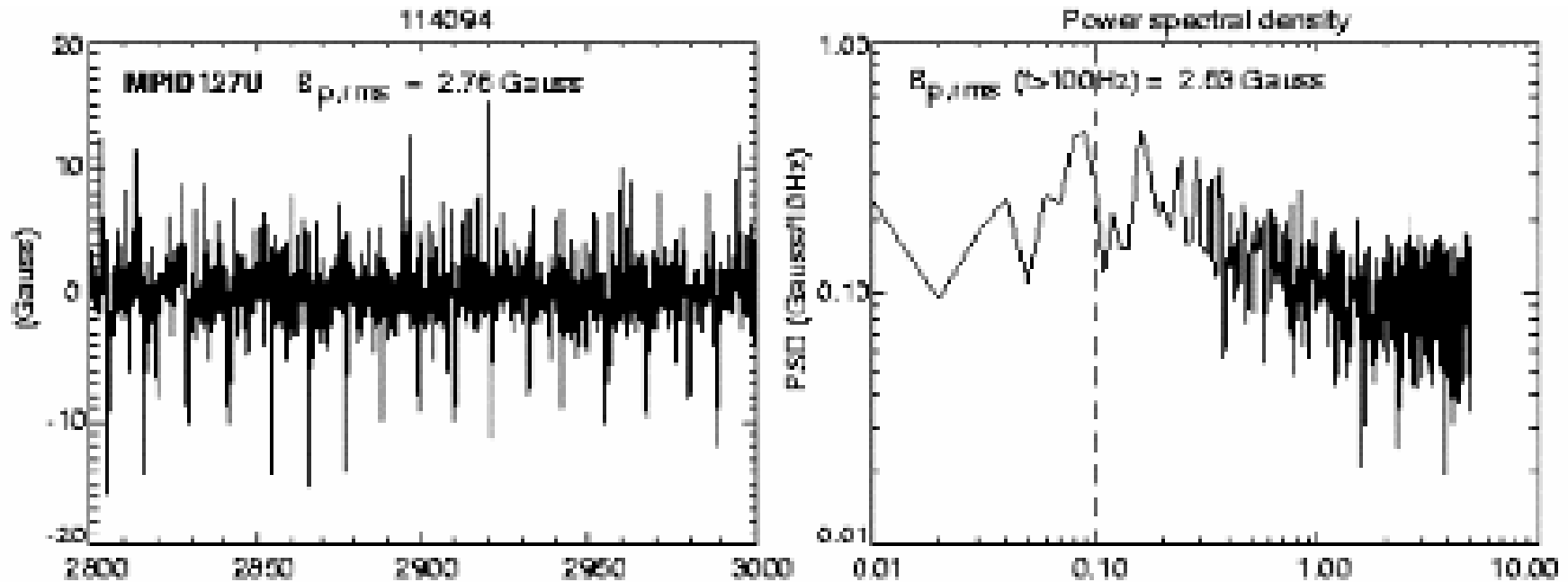


DIII-D New Internal Control Coils are an Effective Tool for Pursuing Active and Passive Stabilizations of the RWM



- Inside vacuum vessel: faster time response for feedback control
- Closer to plasma: more efficient coupling

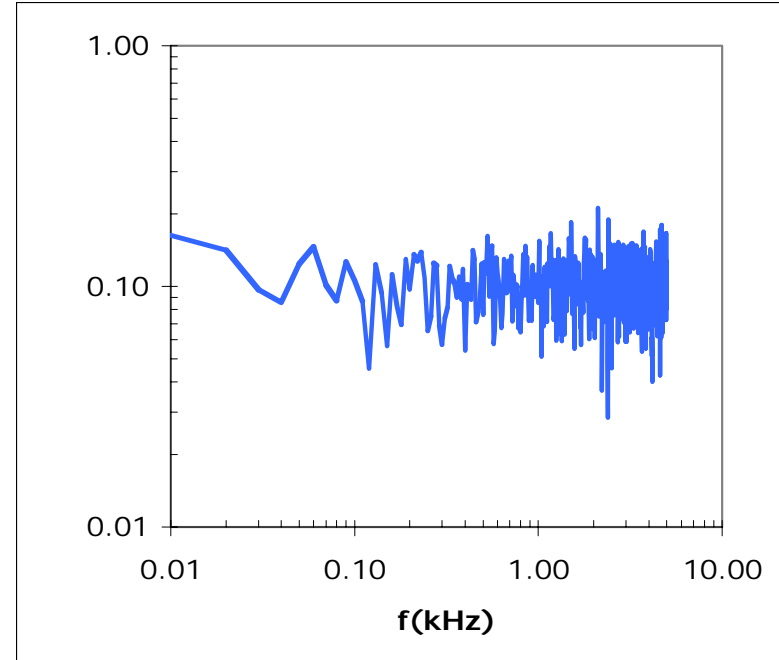
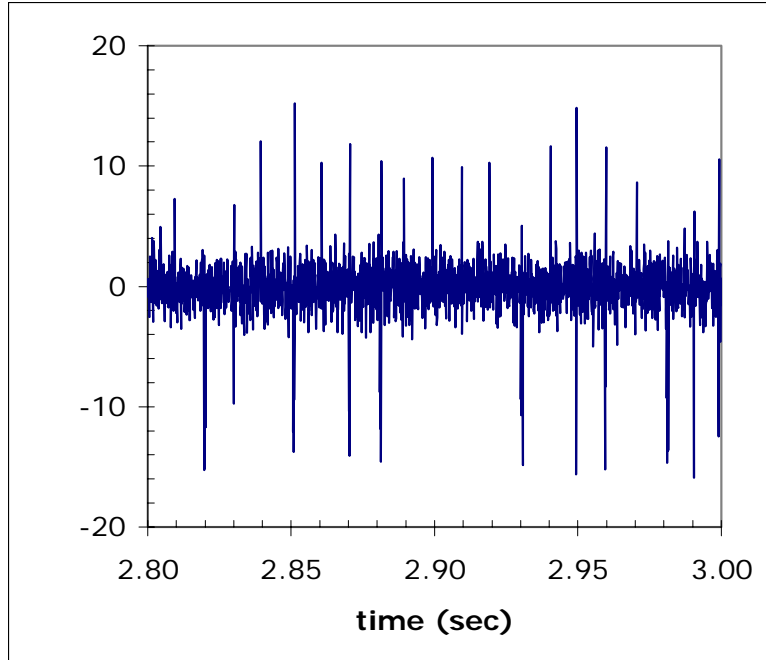
RWM Noise Data on DIII-D



Noise on the poloidal field sensors in the midplane. The signals are corrected for DC offsets. The power spectral density is shown as root-mean square amplitude per 10Hz frequency bin.



Feedback Power Determined by Noise on DIII-D Poloidal Sensors: Broadband and ELMs

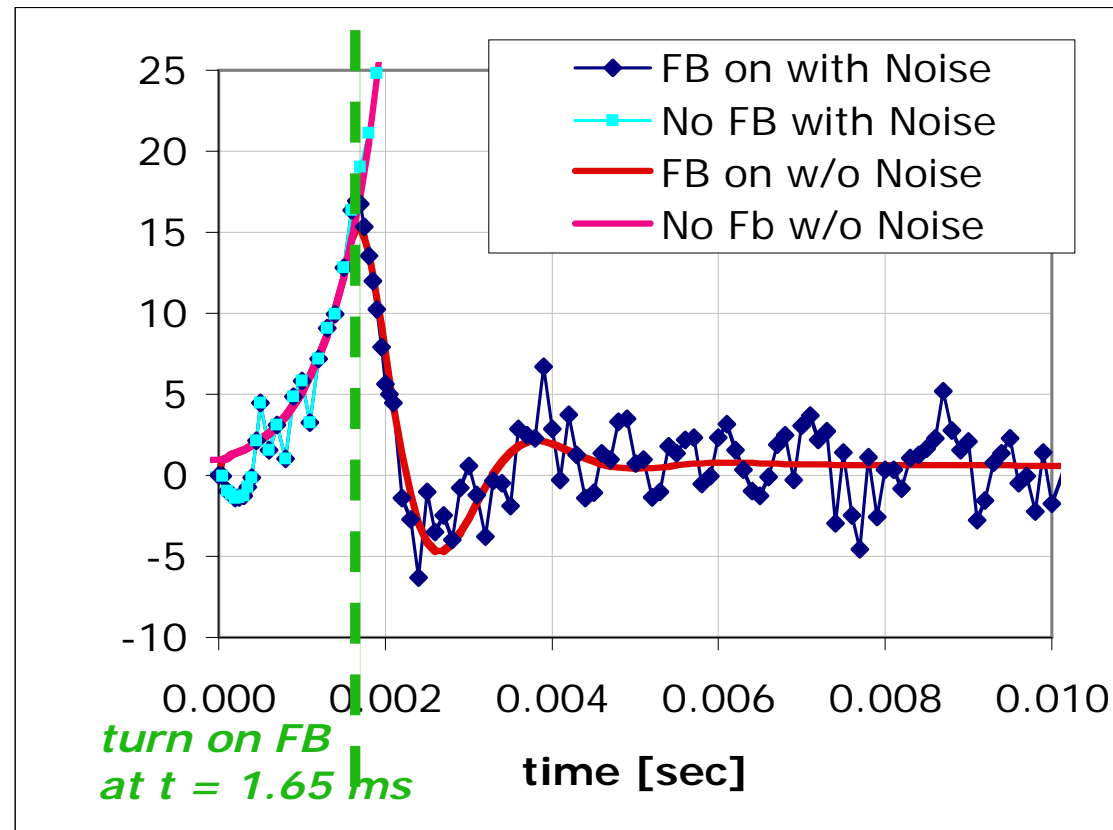


Broadband noise was modeled as Gaussian random number with standard deviation **1.5 G** about 0 mean and frequency 10kHz.

To the broadband noise **ELMs** (Edge Localized Modes) were added as additional Gaussian random distribution from **6 G** to **16 G** approximately every 10 msec with +/- chosen with 50% probability and ELMs duration of **200 μ sec**.



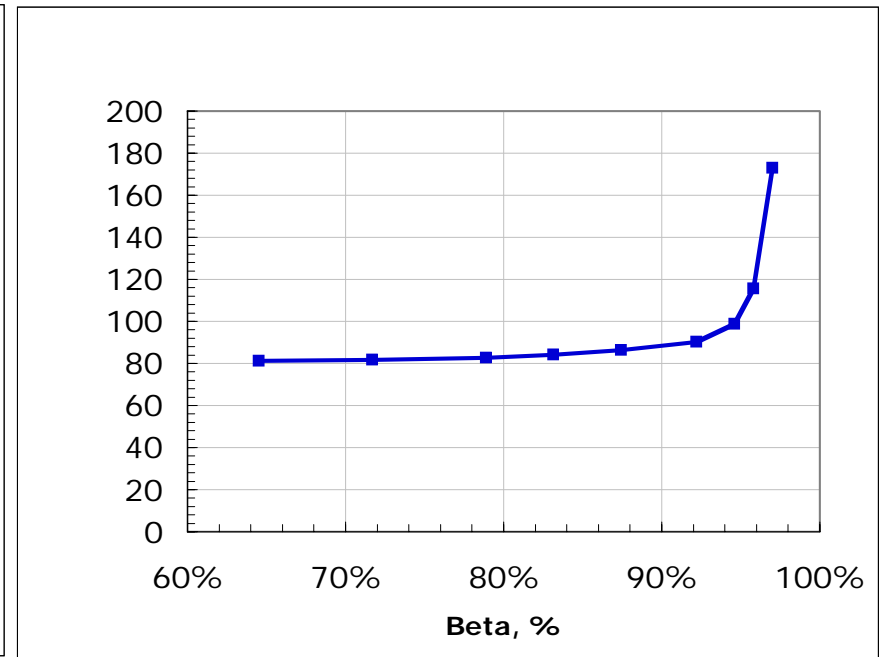
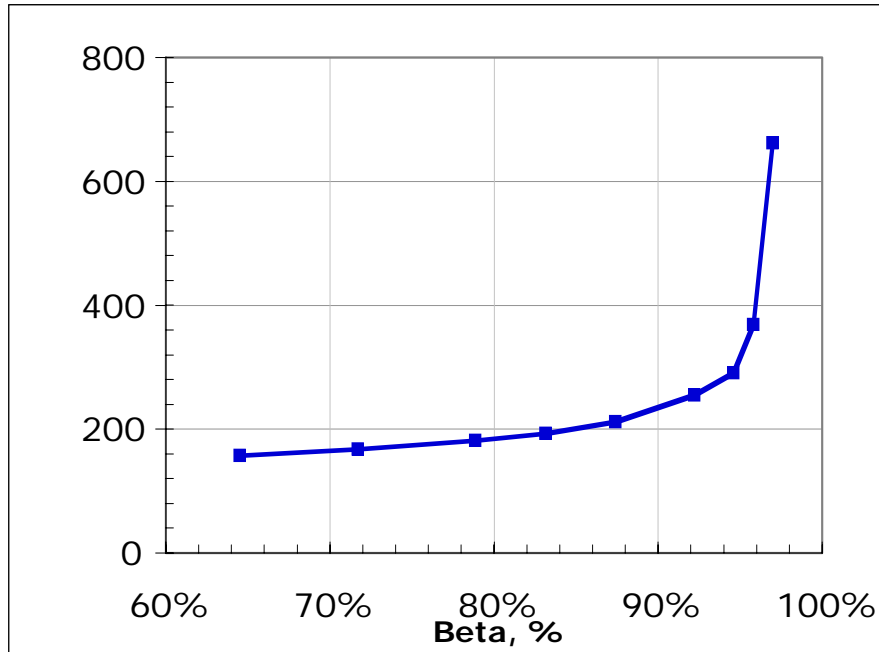
Effects of Noise on Feedback Dynamics



- $L=60\mu\text{H}$ and $R=30\text{m}\Omega$ DIII-D I-Coil Feedback Model with Proportional Gain $G_p=7.2\text{Volts/Gauss}$



Resonant Amplification of Noise Limits Feedback when Approaching Ideal Limit



*Maximum control coil current and voltage
as function of β_{normal}*

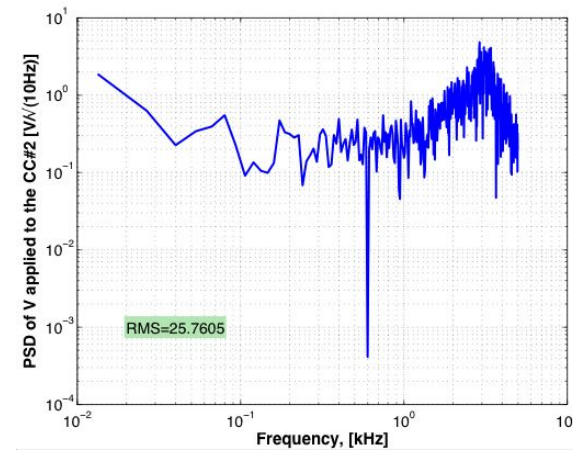
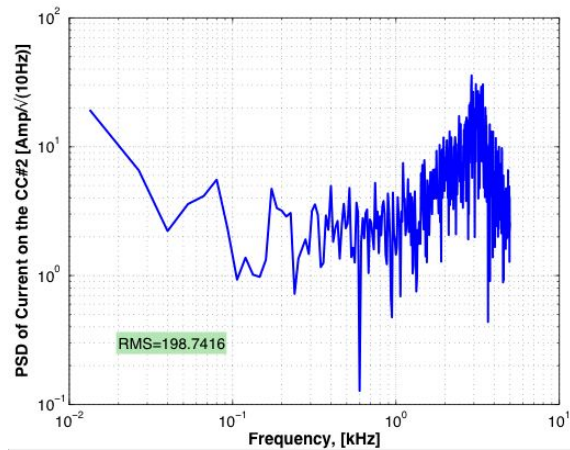
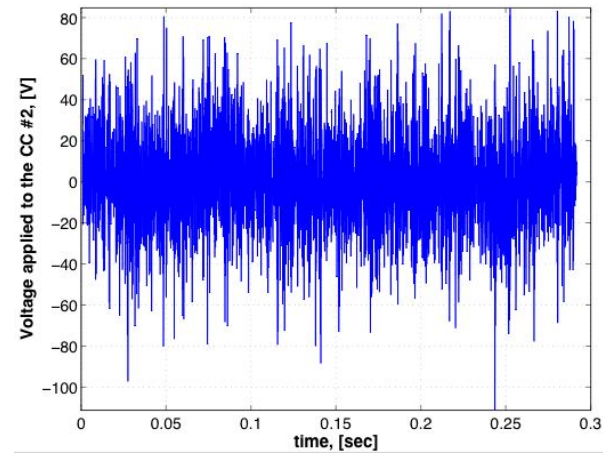
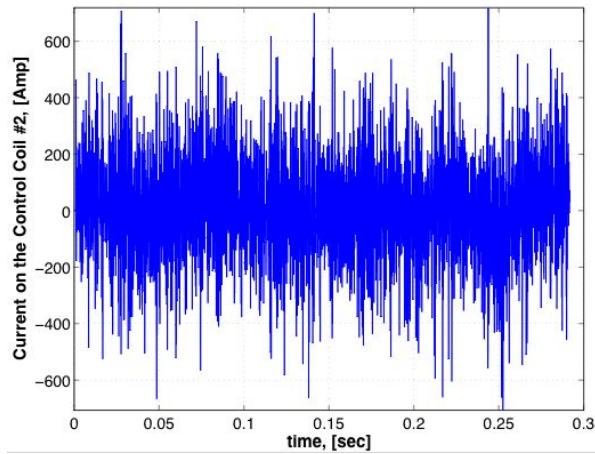


Transient VALEN Runs **with noise** and **time delay** were performed for a range of 3 “coil speeds”

- **High Speed Coil** $R/L = 9.4 \cdot 10^3 \text{ sec}^{-1}$ ($L_{cc}=10.3\mu\text{H}$ & $R_{cc}=97.3\text{mOhm}$) for the $C_\beta=90\%$, time delay $\tau=40 \mu\text{sec}$ and feedback gain $G_p=2.5e+8 \text{ V/Weber}$;
- **Intermediate Speed Coil** $R/L = 2.7 \cdot 10^3 \text{ sec}^{-1}$ ($L_{cc}=9.7\mu\text{H}$ & $R_{cc}=26.03\text{mOhm}$) for the $C_\beta=90\%$, time delay $\tau=65 \mu\text{sec}$ and feedback gain $G_p=6.3e+7 \text{ V/Weber}$;
- **Slow Speed Coil** $R/L = 500 \text{ sec}^{-1}$ ($L_{cc} = 60.\mu\text{H}$ & $R_{cc}=30.\text{mOhm}$) for the $C_\beta=90\%$, time delay $\tau=65 \mu\text{sec}$ and feedback gain $G_p=1.e+8 \text{ V/Weber}$.



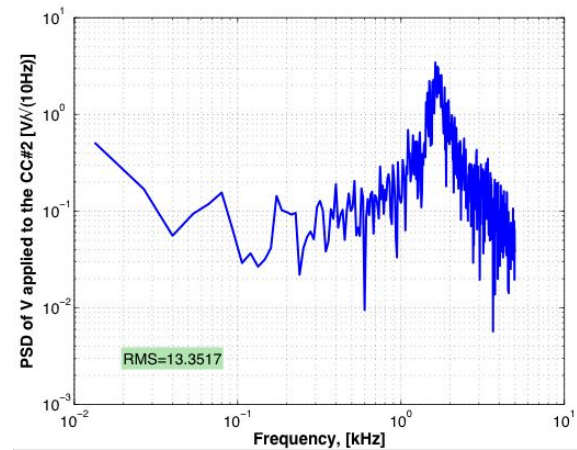
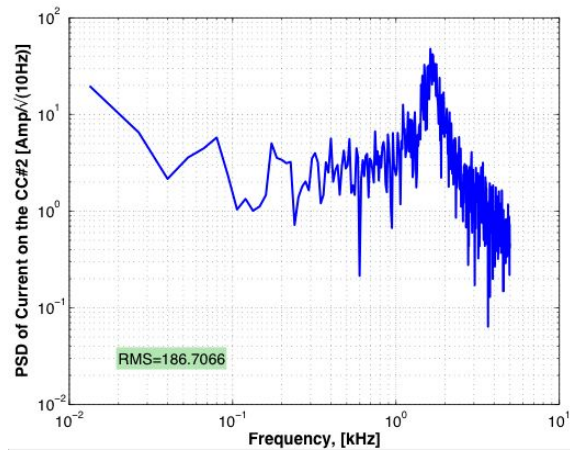
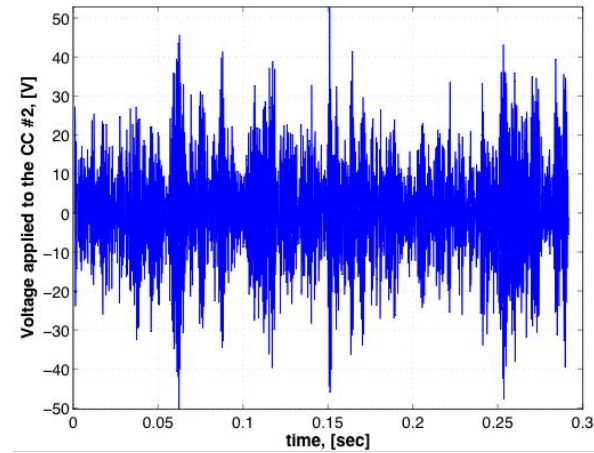
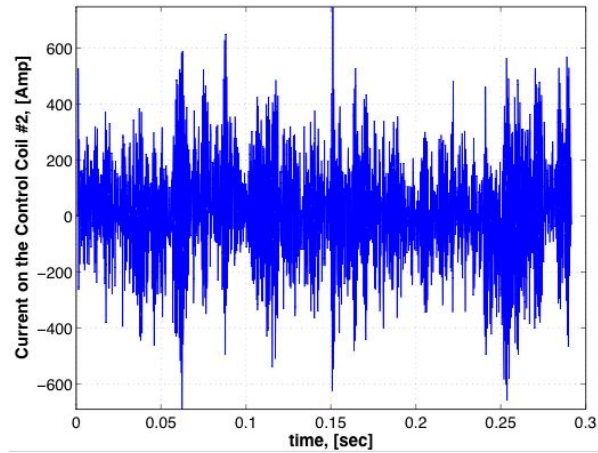
High Speed Coil $C_{\beta}=90\%$, $G_p=2.5e+8$ V/Weber, $\tau=40 \mu\text{sec}$



- Power Spectrum Density for the current control coil #2 has peak around 3kHz that corresponds to the frequency calculation (J.Bialek)



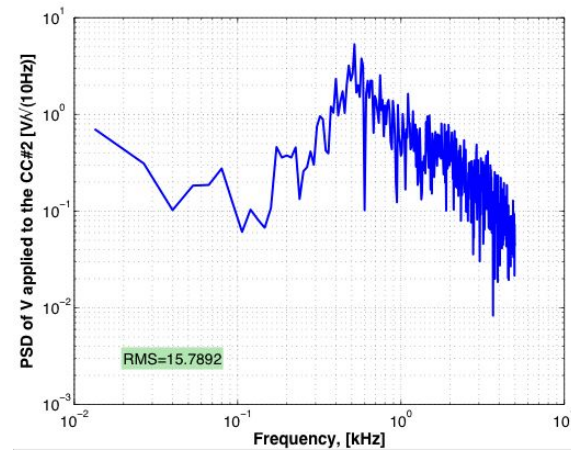
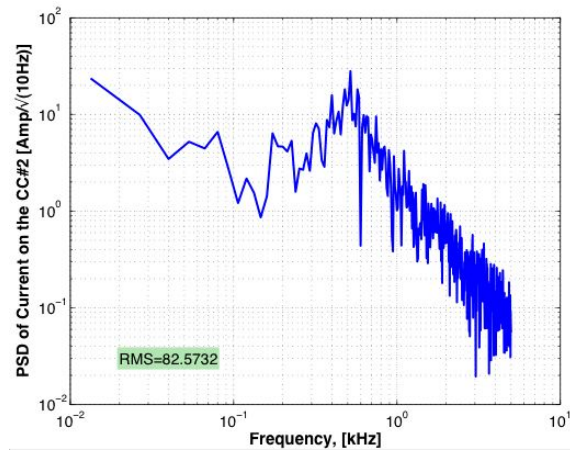
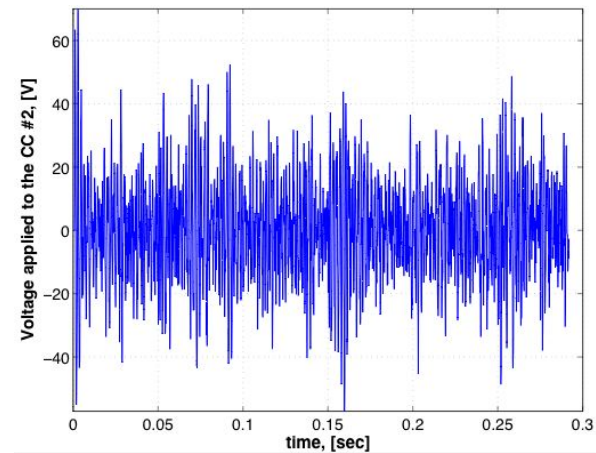
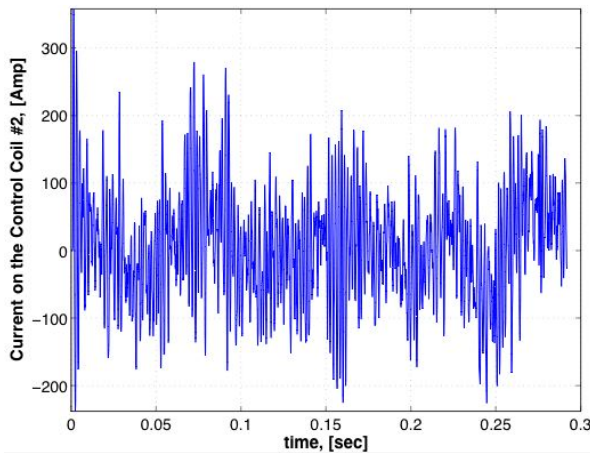
Intermediate Speed Coil $C_\beta=90\%$, $G_p=6.3e+7$ V/Weber, $\tau=65$ μsec



- Power Spectrum Density for the current control coil #2 has peak around 1.8 kHz that corresponds to the frequency calculation (J.Bialek)



Slow Speed Coil $C_\beta=90\%$, $G_p=1.e+8$ V/Weber, $\tau=65 \mu\text{sec}$



- Power Spectrum Density for the current control coil #2 has peak around 0.4-0.5kHz that corresponds to the frequency calculation (J.Bialek)

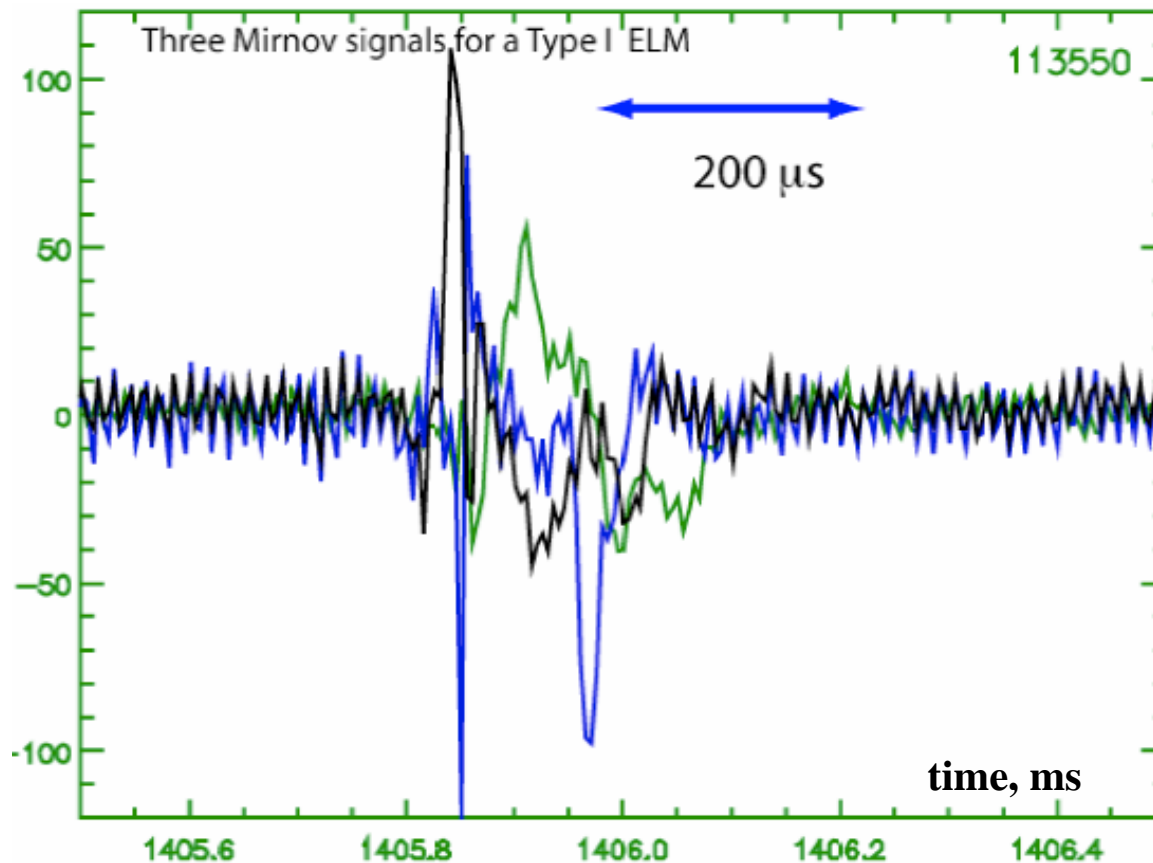


Estimated Power Requirements for DIII-D

	RMS of I [Amp]	RMS of V [V]	Peak Power [kWatt]	RMS of Power [kWatt]
High Speed coil	198.7	25.8	61.9	6.4
Intermediate speed coil	186.7	13.4	25.1	3.0
Slow speed coil	82.5	15.7	14.3	1.4



Magnetic Interference From ELMs Occurs on a Shorter Time Scale Than ELM D_{α} emission

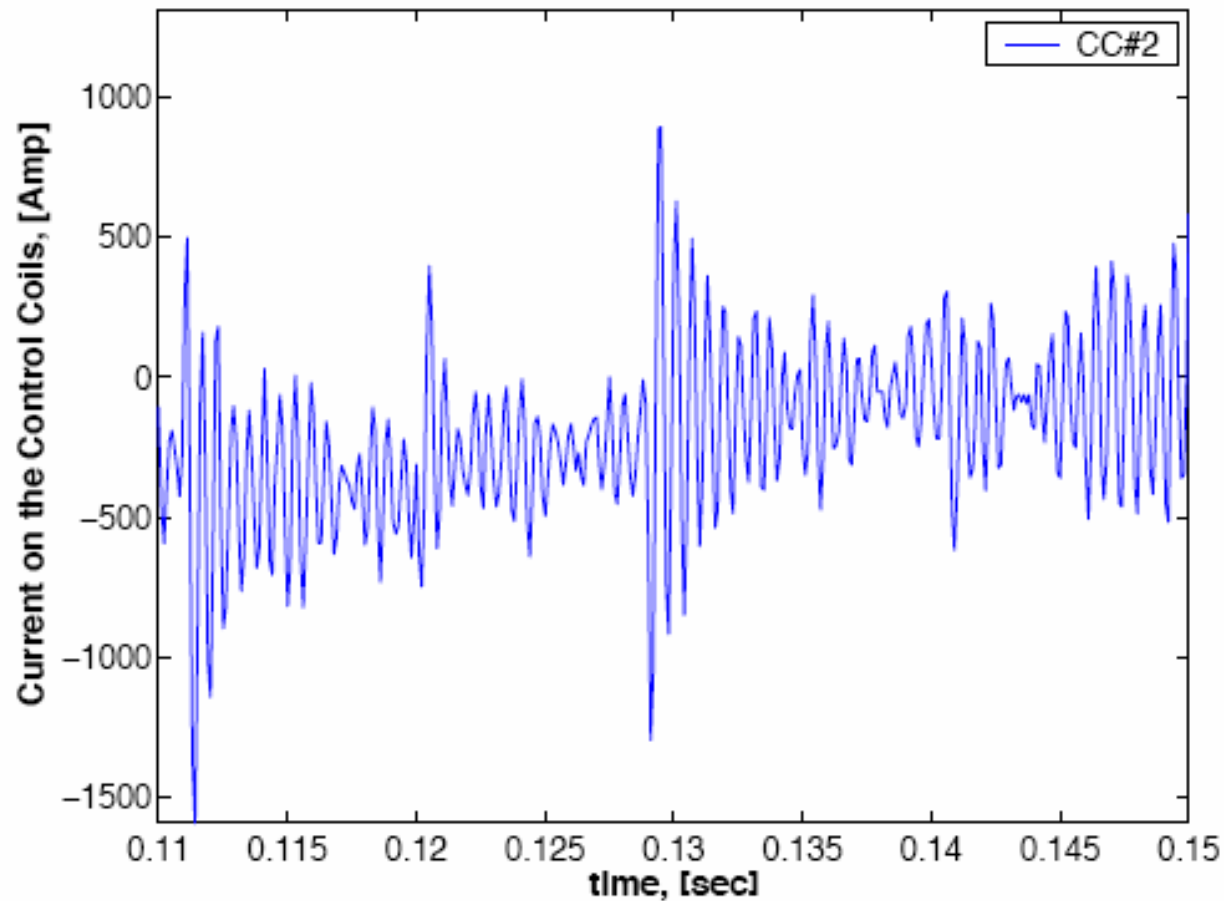


Okabayashi, 5/04

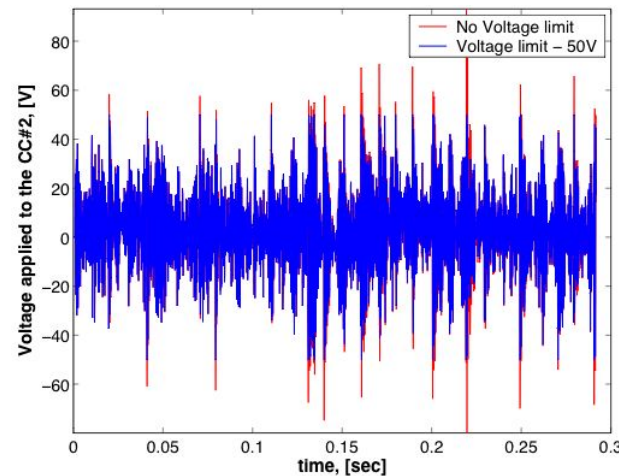
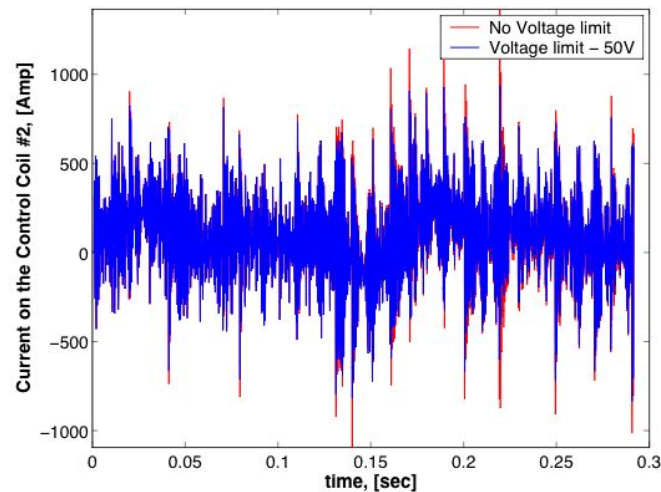
- Main activity takes place within 50μ s leading to relaxation
- Gating off 50μ s of feedback may be sufficient



ELM Response of Feedback Loop Results in No Loss of RWM Control



Intermediate Speed Coil Coil $C_\beta=90\%$, $G_p=6.3e+7$ V/Weber, $\tau=65$ μ sec, ELMs lasting 200 μ sec and **Voltage Limit 50 V.**

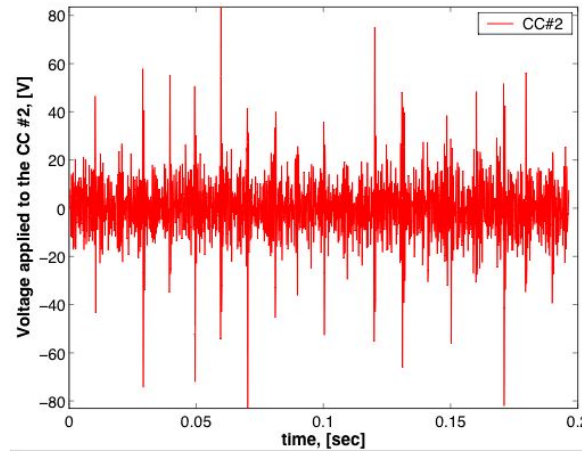
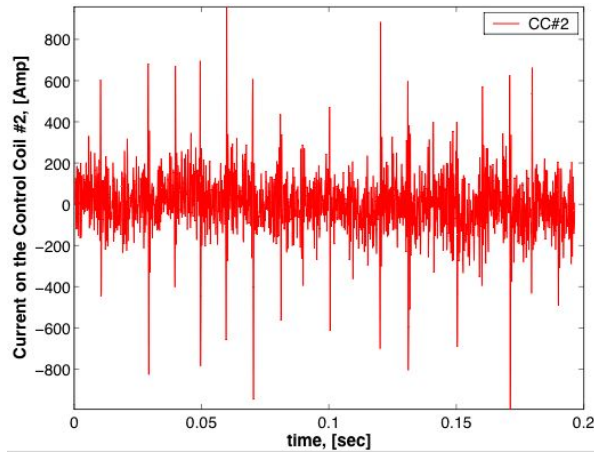


	RMS of I [Amp]	RMS of V [Volts]	Peak Power [kWatt]	RMS of Power [kWatt]
No Voltage Limits	270.9	18.1	73.8	6.7
Voltage limits 50V	260.6	17.1	40.7	5.6

Restrictions of 50 V on voltages do not effect feedback performance.



Intermediate Speed Coil $C_\beta=93.6\%$,
 $G_p=7.9e+8$ V/Weber, $\tau=10$ μ sec, ELMs lasting 200 μ sec
 and **low pass filter 20kHz.**

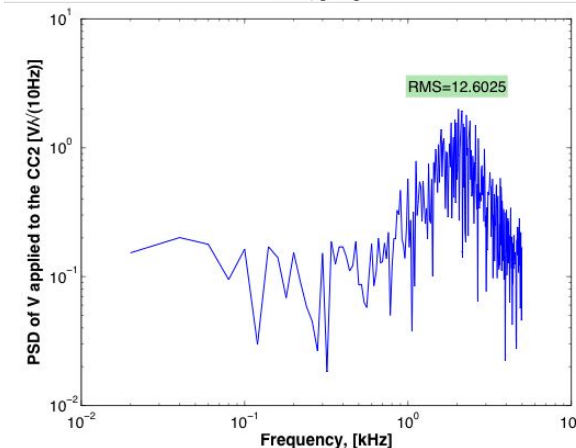
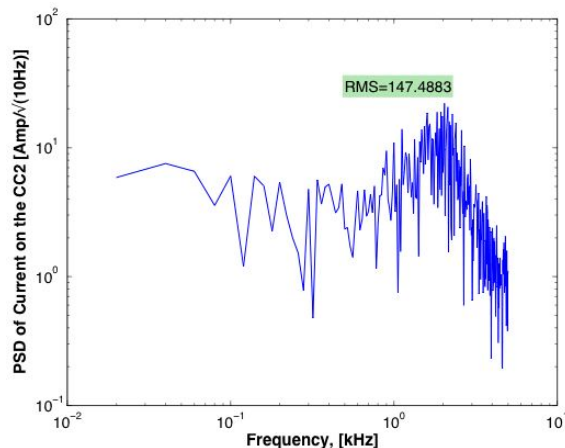


Current [Amp]

Peak Value	RMS
957.9	142.5

Applied Voltage [V]

Peak Value	RMS
83.5	12.6

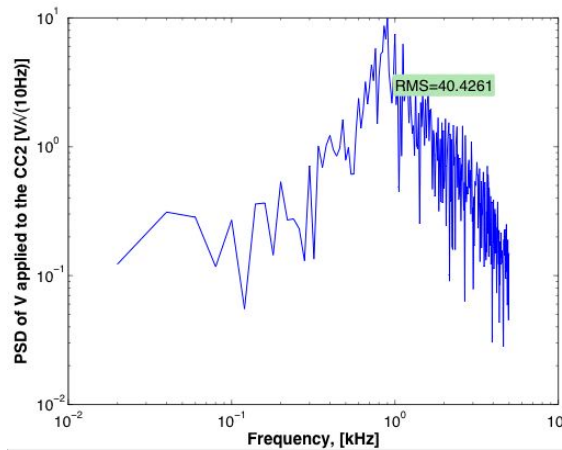
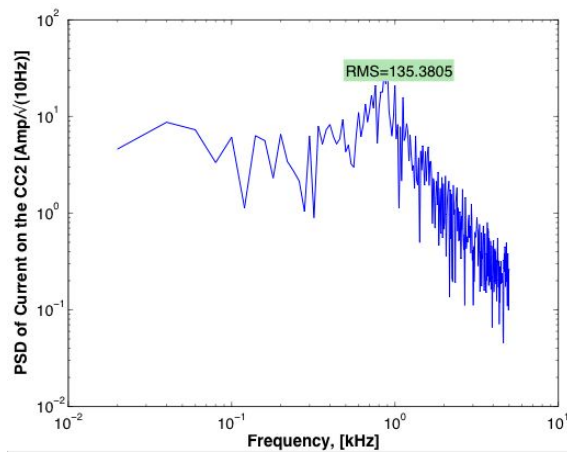
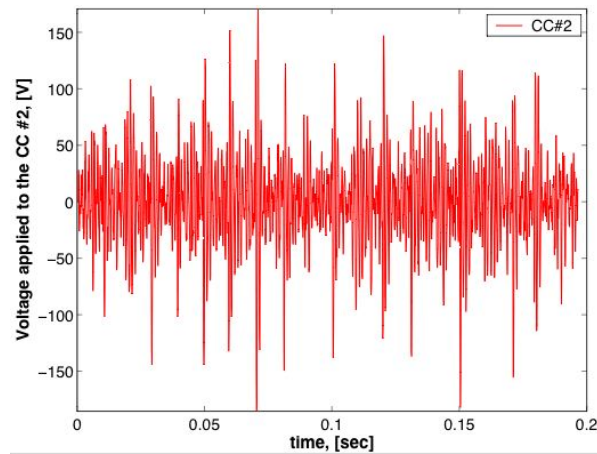
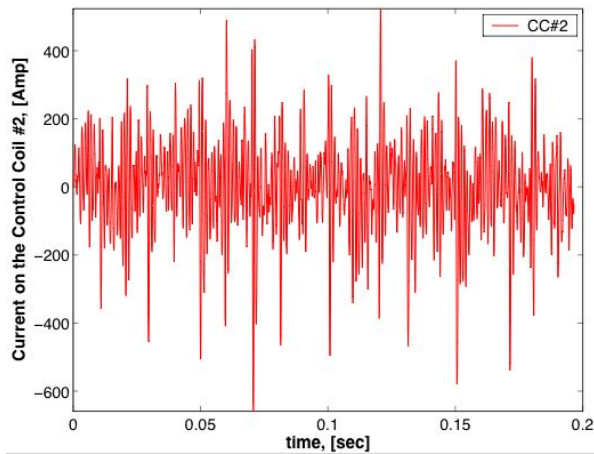


Power [kWatts]

Peak Value	RMS
40.9	3.04



**Slow Speed Coil Coil $C_\beta=93.6\%$,
 $G_p=1.6e+8$ V/Weber, $\tau=10 \mu\text{sec}$, ELMs lasting $200 \mu\text{sec}$
 and **low pass filter 20kHz****



Current [Amp]

Peak Value	RMS
523	135.4

Applied Voltage [V]

Peak Value	RMS
170.8	40.4

Power [kWatts]

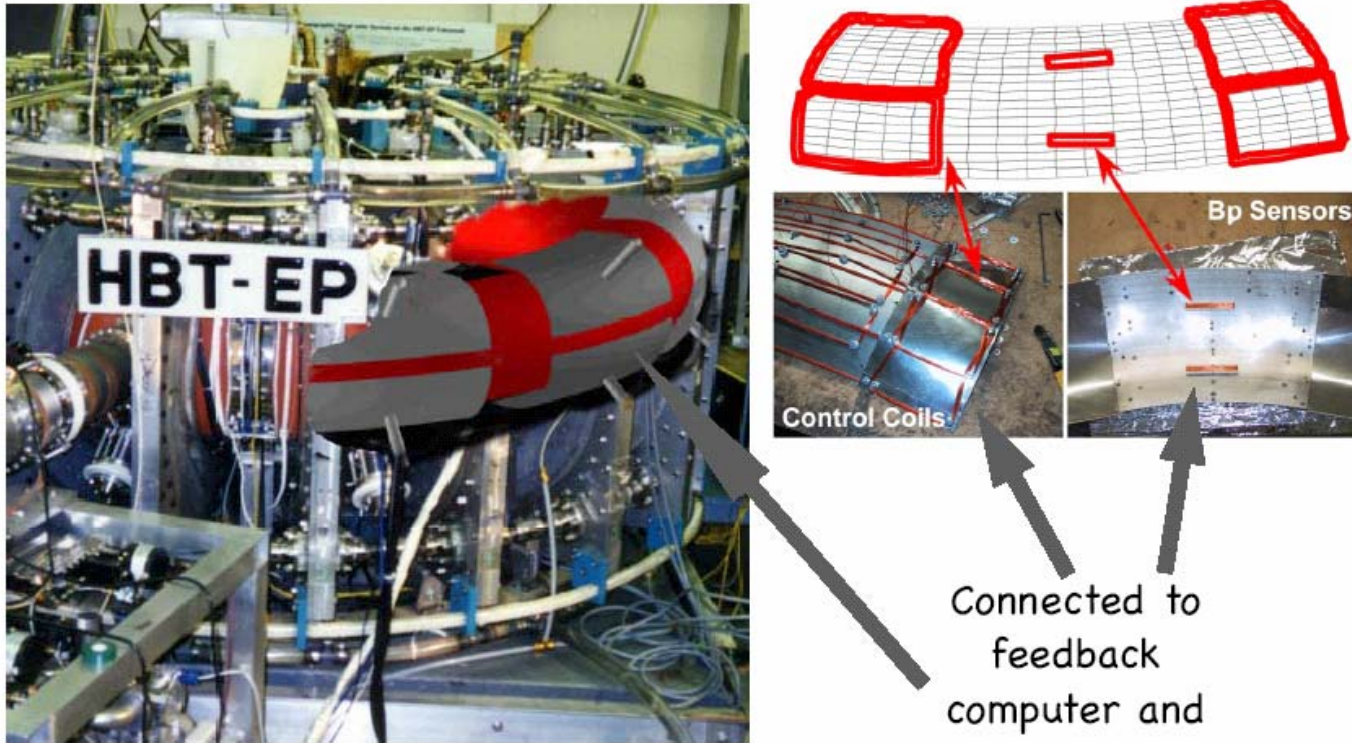
Peak Value	RMS
72	7.1



Time dependent problem for **HBT-EP with
time delay and band pass filter**



HBT-EP: Adjustable Wall & Modular Coils



Major radius: $R_o = 0.92-0.97$
Plasma current: $I_p \leq 25$ kA
Pulse length: $\tau \sim 10$ ms
Density: $\langle n_e \rangle \sim 1 \times 10^{19} \text{ m}^{-3}$

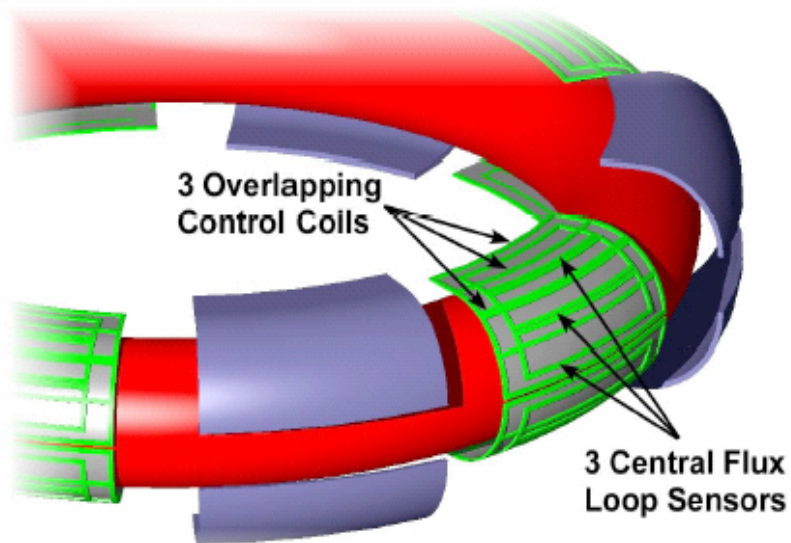
Minor radius: $a = 0.15-0.19$ m
Toroidal field: $B_T \leq 3.3$ kG
Temperature: $\langle T_e \rangle \sim 80$ eV

Connected to
feedback
computer and
control amps

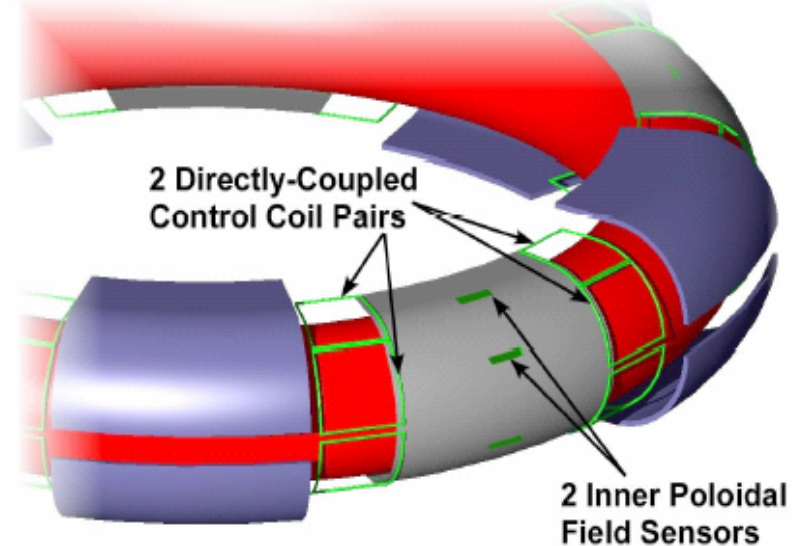


New “Mode Control” Sensor Coils

(a) Previous “Smart Shell” Sensor/Control Coils



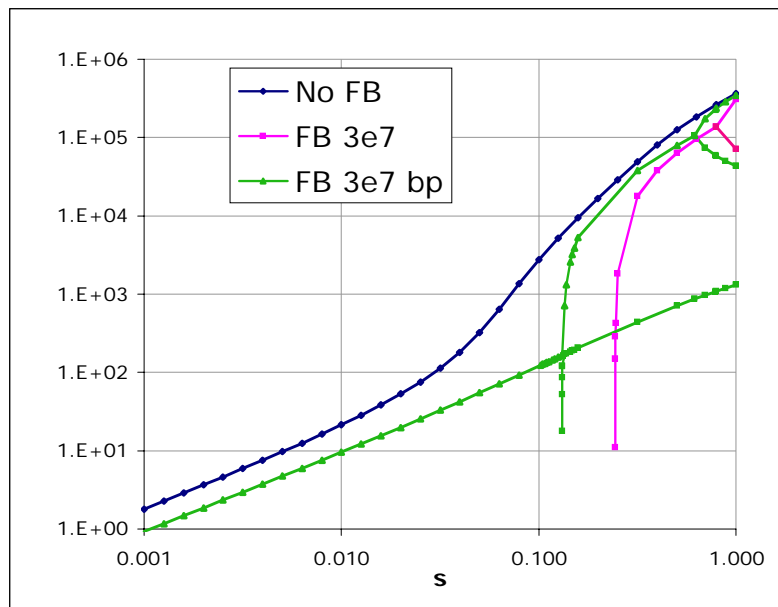
(b) New “Mode Control” Sensor/Control Coils



- Eliminate unwanted coupling between mode sensor and control coils.
- Emphasize direct coupling between plasma and control coils while minimize coupling to stabilizing wall



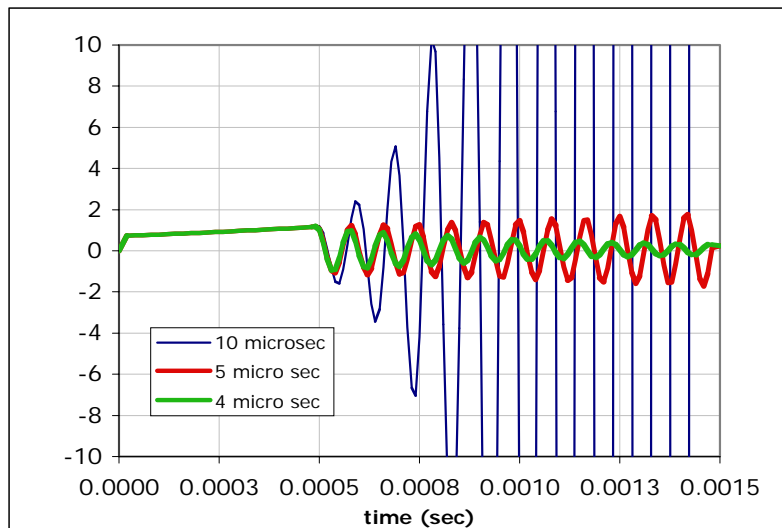
Transient calculations for basic HBT geometry with feedback



- HBT with 8/10 aluminum shells out 4 cm.
- with $G_p = 3.85E+07$. A single B_p sensor was used to drive 20 control coils.
- Band pass filters:
 - low frequency cut off 300Hz ($R_l=1.5\text{Ohm}$ and $L_l=796.2 \mu\text{H}$);
 - high frequency cut off 25 kHz ($R_h=125\text{Ohm}$ and $L_h=796.2 \mu\text{H}$).



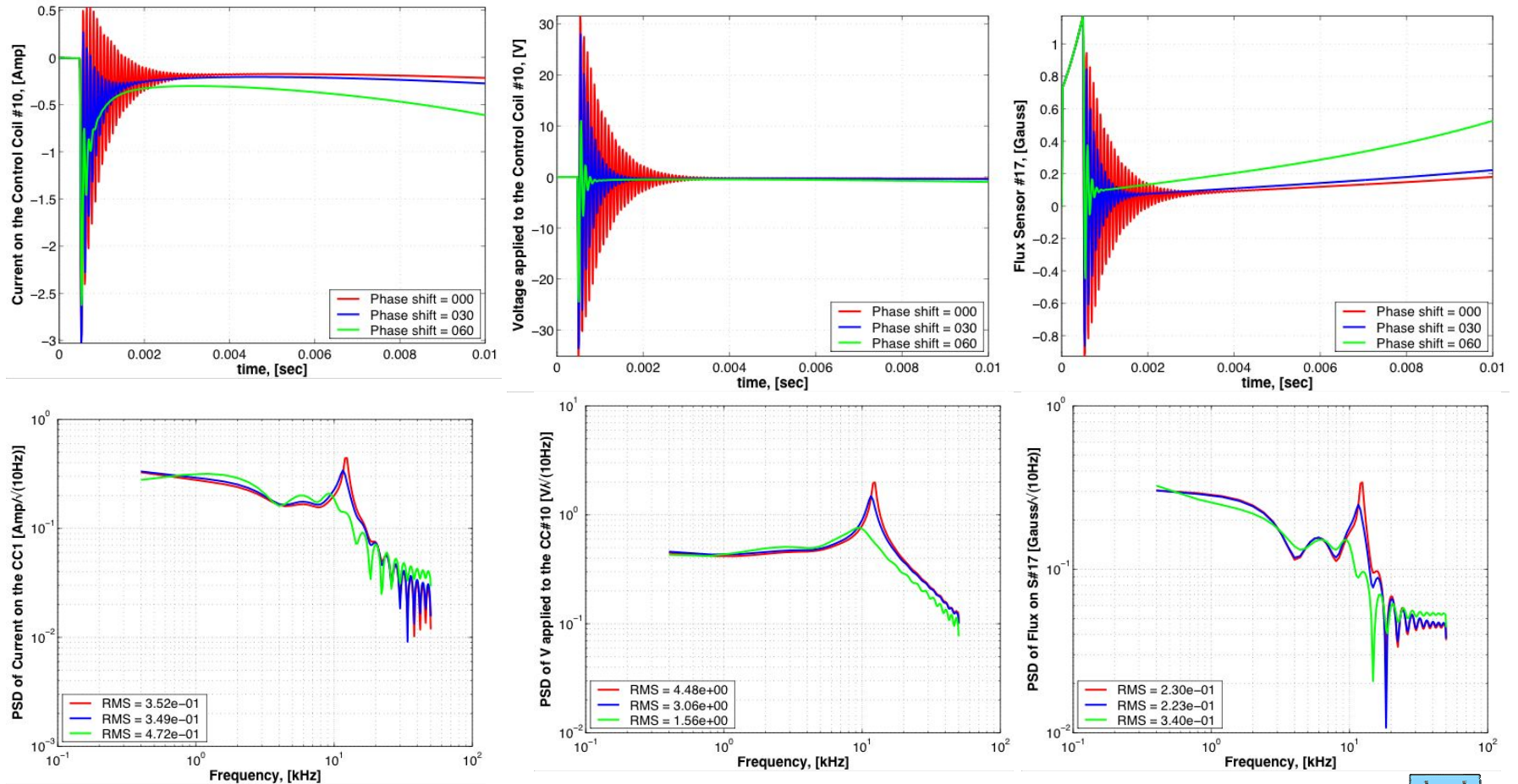
Time delay in HBT model with band pass filters for $s = 0.072346$



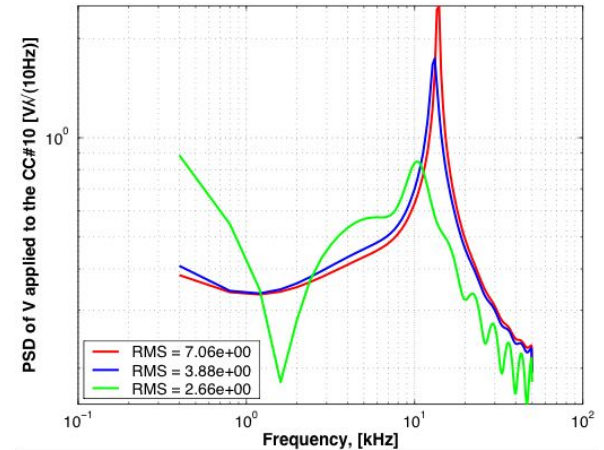
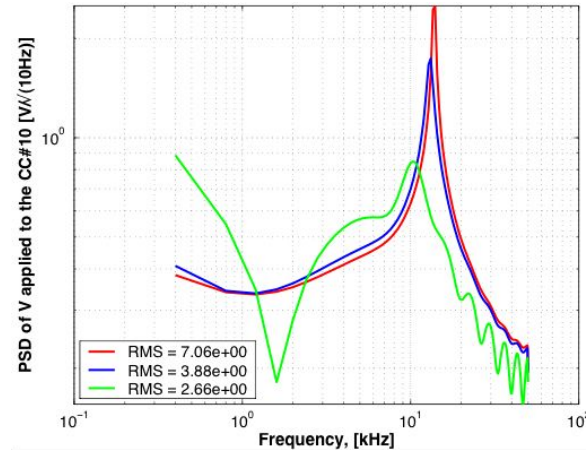
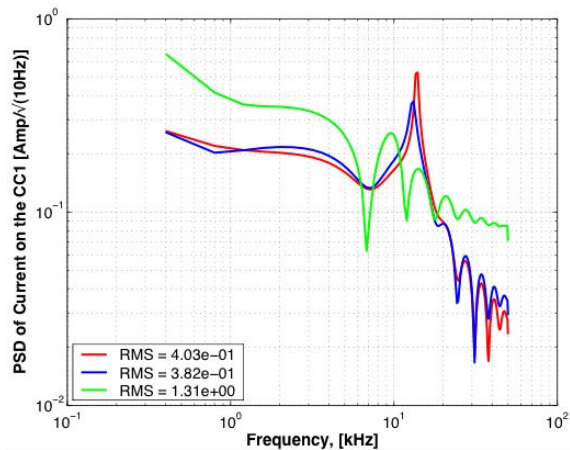
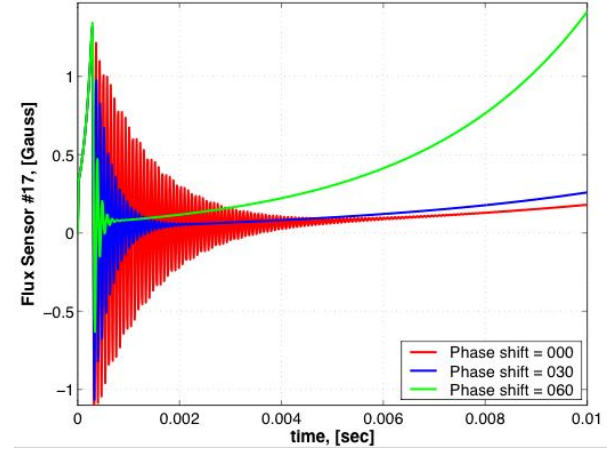
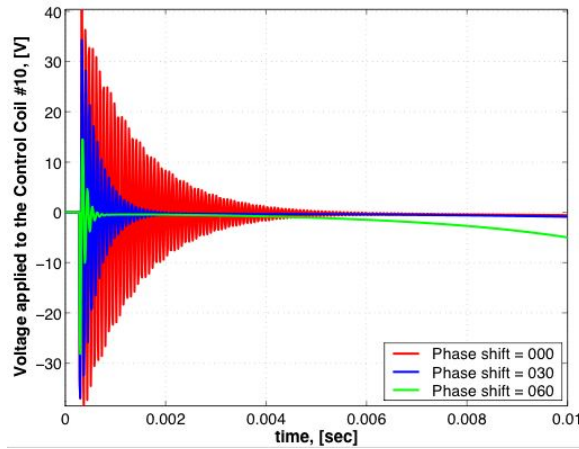
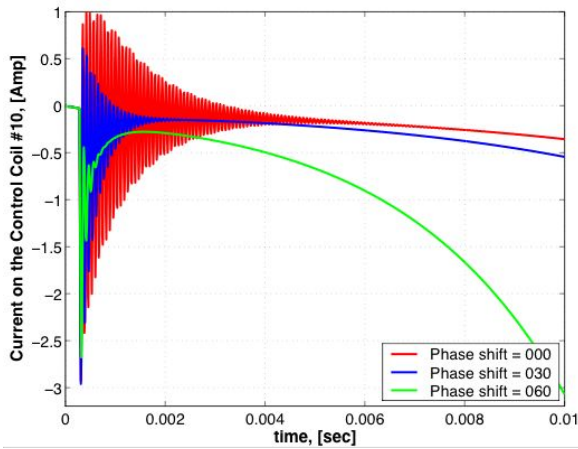
- VALEN showed that time delay of $\tau = 10 \mu\text{sec}$ and $\tau = 5 \mu\text{sec}$ are unstable
- Time delay of $4 \mu\text{sec}$ is stable.



Case #1. $s = 0.072346$ (passive growth rate of $1.e+3$) with time delay $\tau = 4 \mu\text{sec}$



Case #2. $s = 0.12589$ Passive growth rate of $5.22e+3$ time delay $\tau = 0.5 \mu\text{sec}$



Conclusions and Future Work

- Sensor noise and time delays were successfully modeled in RWM feedback system of DIII-D. Feedback power requirements and system performance limits were estimated, including the RMS and power spectral density of control coil current and voltage for the feedback configurations.
- Analysis of the effects of ELMs on the DIII-D RWM feedback control system shows no loss of control during ELM events, even if the amplifier is briefly saturated.
- These RWM control modeling studies also show that significantly more power is required to suppress the RWM as the ideal wall limit is approached, due to resonant amplification of the noise applied through the control coils.
- VALEN modeling of HBT model, with bandpass filters and time delay, was performed for different phase shifts in feedback. This is work in progress, as calculated time delay limits (4 μ sec) differ from experimental (10 μ sec), whereas implemented phase shift calculations confirm expected feedback deterioration at greater angles.

